Published in final edited form as:
Cell. 2008 July 25; 134(2): 279–290. doi:10.1016/j.cell.2008.06.017.

Superoxide Flashes in Single Mitochondria

Wang Wang[1], **Huaqiang Fang**[2], **Linda Groom**[3], **Aiwu Cheng**[4], **Wanrui Zhang**[2], **Jie Liu**[2], **Xianhua Wang**[2], **Kaitao Li**[2], **Peidong Han**[2], **Ming Zheng**[2], **Jinhu Yin**[5], **Weidong Wang**[5], **Mark P. Mattson**[4], **Joseph P. Y. Kao**[6], **Edward G. Lakatta**[1], **Shey-Shing Sheu**[3], **Kunfu Ouyang**[7], **Ju Chen**[7], **Robert T. Dirksen**[3], and **Heping Cheng**[2]

1*Laboratory of Cardiovascular Sciences, National Institute on Aging, National Institutes of Health, Baltimore, Maryland 21224, USA*

2*Institute of Molecular Medicine and National Laboratory of Biomembrane and Membrane Biotechnology, Peking University, Beijing 100871, China*

3*Department of Pharmacology and Physiology, University of Rochester, School of Medicine and Dentistry, Rochester, New York 14642, USA*

4*Laboratory of Neurosciences, National Institute on Aging, National Institutes of Health, Baltimore, Maryland 21224, USA*

5*Laboratory of Genetics, National Institute on Aging, National Institutes of Health, Baltimore, Maryland 21224, USA*

6*Department of Physiology, University of Maryland School of Medicine, Baltimore, Maryland 21201, USA*

7*Department of Medicine, University of California, San Diego, California 92093, USA*

SUMMARY

The mitochondrion is the primary source of reactive oxygen species (ROS) in eukaryotic cells. With the aid of a novel mitochondrial matrix-targeted superoxide indicator, here we show that individual mitochondria undergo spontaneous bursts of superoxide generation, termed “superoxide flashes”. Superoxide flashes occur randomly in space and time, exhibit all-or-none properties, and reflect elementary events of superoxide production within single mitochondria across a wide diversity of cells. Individual flashes are triggered by transient openings of the mitochondrial permeability transition pore (mPTP) and are fueled by electron transfer complexes-dependent superoxide production. While decreased during cardiac hypoxia/anoxia, a flurry of superoxide flash activity contributes to the destructive rebound ROS burst observed during early reoxygenation after anoxia. The discovery of superoxide flashes reveals a novel mechanism for quantal ROS production by individual mitochondria and substantiates the central role of mPTP in oxidative stress related pathology in addition to its well-known role in apoptosis.

INTRODUCTION

Reactive oxygen species (ROS) are a class of radical or non-radical oxygen-containing molecules that display high reactivity with lipids, proteins and nucleic acids. Depending on concentration, location and context, ROS can be either “friends” or “foes”. Excessive ROS

Address Correspondence to H.C. (chengp@pku.edu.cn) or W.W. (wangwang@umich.edu).

generation leads to apoptotic and necrotic cell death (Brookes et al., 2004; Dypbukt et al., 1994) and pathogenesis of a panel of clinically distinct disorders including neurodegeneration (e.g. Alzheimer's disease), atherosclerosis, diabetes and cancer (Andersen, 2004; Dhalla et al., 2000; Klaunig and Kamendulis, 2004). Accumulative and systemic ROS damage also underlies cell senescence and aging (Beckman and Ames, 1998). However, increasing evidence indicates that homeostatic and physiological levels of ROS are indispensable in regulating diverse cellular processes including ion channel/transporter function (Zima and Blatter, 2006), Ca^{2+} spark production (Isaeva et al., 2005; Yan et al., 2008), protein kinase/phosphatase activation, and gene expression (Droege, 2002). The emerging view is that ROS contribute to multiple essential intracellular signaling processes ranging from cell metabolism to ischemic preconditioning (Droege, 2002; Otani, 2004).

In quiescent cells, ROS are primarily produced as byproducts of mitochondrial respiration when electrons leak from the electron transfer chain (ETC) (Wallace, 2001a, b). Superoxide anion ($O_2^{\cdot-}$) is the primary ROS generated by the ETC and is dismutated to hydrogen peroxide (H_2O_2) either spontaneously or by superoxide dismutase (SOD). Recent studies have demonstrated massive increases in localized ROS production during metabolic stress (Romashko et al., 1998), photostimulation (Zorov et al., 2000), and excessive elevations in intracellular ROS or Ca^{2+} (Duchen, 2000; Vercesi et al., 1997) that ultimately contribute to necrotic or apoptotic cell death.

The present study reports the surprising discovery of a quantal mode of mitochondrial ROS production under resting conditions in diverse cell types. The development of a highly sensitive superoxide indicator with high-contrast and reversible kinetics enables real-time imaging of superoxide production at the level of single mitochondria, and uncovers individual, ~10 second long superoxide-producing events within the mitochondrial matrix. Such quantal mitochondrial ROS production events are controlled by a novel functional coupling between the mitochondrial permeability transition pore (mPTP) and the complexes of ETC. Moreover, we demonstrate that superoxide flash events contribute to increased oxidative stress during cardiac ischemia-reperfusion injury and represent a target of pharmacological preconditioning.

RESULTS

Characterization of a Novel Superoxide Indicator

ROS exist in many different interconvertable forms (e.g. H_2O_2, $O_2^{\cdot-}$, hydroxyl radical, peroxynitrite, etc). The paucity of species-specific and reversible probes for ROS detection in living cells has seriously limited molecular investigations of ROS signaling dynamics. By serendipity, we found that a circularly permuted yellow fluorescent protein (cpYFP), previously used as the core structure for the Ca^{2+} indicator pericam (Nagai et al., 2001), is a novel biosensor for $O_2^{\cdot-}$, the primal ROS generated by the ETC. The fluorescence emission (at 515 nm) of purified cpYFP when excited at 488 nm is five times brighter under strong oxidizing conditions (1 mM aldrithiol) compared to strong reducing conditions (10 mM reduced DTT, Figure 1A), indicative of a large dynamic range. Extensive *in vitro* experiments revealed the superoxide selectivity of cpYFP over other physiologically relevant oxidants and metabolites (Figure 1 and S1). Compared to the fully reduced state, cpYFP fluorescence displays a 250% increase by oxygenation and a full 420% increase by $O_2^{\cdot-}$ (generated by 2 mM xanthine and 20 mU xanthine oxidase under aerobic conditions, Figure 1B). The $O_2^{\cdot-}$ associated increase in cpYFP fluorescence is completely reversed by subsequent addition of Cu/Zn-superoxide dismutase (SOD, 600 U/ml) or prevented by prior addition of SOD (Figure 1B and Figure S1A).

By contrast, cpYFP emission is unchanged by H_2O_2 (0.1–10 mM, Figure 1C) and peroxynitrite (Figure S1B), and is decreased by hydroxyl radical (Figure 1C) and nitric oxide (Figure S1C).

Other metabolites tested, including physiological levels of Ca^{2+}, ATP, ADP, $NAD(P)^+$, and NAD(P)H, all exert negligible or only marginal effects (Figure 1D, 1E, Figure S1D and S1E). Unlike GFP-based redox biosensors (Hanson et al., 2004; Ostergaard et al., 2001), the fluorescence emission of cpYFP is unaltered when the redox potential varies between −319 mV and −7.5 mV (produced by differential mixing of reduced and oxidized DTT, Figure 1F). As would be expected of a fluorescent protein-based indicator (Belousov et al., 2006; Nagai et al., 2001), cpYFP emission is brighter in an alkaline environment, such as that within the mitochondrial matrix (pH ~8.0, Figure S1F). These results indicate that cpYFP can be judiciously used as a genetically encoded biosensor of superoxide anions. Compared to mito-SOX, an ethidium bromide (EB) derivative that reacts with $O_2^{\cdot-}$ and then fluoresces upon irreversible binding to mitochondrial DNA, a major advantage of cpYFP is its reversibility that permits real-time measurements of dynamic changes in superoxide levels in living cells (see below).

Mitochondrial Superoxide Flashes in Living Cells

We employed adenovirus-mediated gene transfer to express cpYFP in the mitochondrial matrix of cultured adult cardiac myocytes using the cytochrome C oxidase subunit IV (COX IV) targeting sequence (mt-cpYFP). Confocal imaging revealed that mt-cpYFP stains bundle-like subcellular structures punctuated at Z-lines of the sarcomere (Figure 2A), in agreement with the known spatial organization of cardiac mitochondria (Ramesh et al., 1998). Strikingly, localized and transient “flashes” of mt-cpYFP fluorescence occur stochastically amidst a quiescent background in resting cardiomyocytes (Figures 2A, 2B and supplemental movie). A typical flash rises abruptly, peaks in 3.5 ± 0.1 s, and dissipates with a half time of 8.6 ± 0.2 s (n = 409 flashes from 53 cells, Figures 2B, 2H and 2I). The average fractional peak increase of mt-cpYFP fluorescence ($\Delta F/F_0$) during a flash is 0.41 ± 0.02 (Figure 2G); the top 10% brightest events display a $\Delta F/F_0$ of 1.0 ± 0.1 (n = 41), which most likely reflects the true amplitude without out-of-focus blurring. While mitochondrial flashes occur randomly in space and time, individual events are sharply confined to tiny elliptical areas each spanning 0.94 ± 0.01 μm laterally and 1.68 ± 0.03 μm longitudinally (n = 409). These results indicate that a flash arises from a single or pair of functionally coupled mitochondria. The quiescence of adjacent mitochondria during a flash (Figure 2A) indicates that mitochondrial flashes do not propagate under normal experimental conditions.

Because a 5-fold increase in scanning laser intensity did not elevate the rate of flash production (Figure S2), spontaneous mitochondrial flashes are not due to phototoxicity. Moreover, experiments using a mitochondrial-targeted EYFP as a pH biosensor (Takahashi et al., 2001) fail to detect transient events of mitochondrial alkalinization with a similar frequency and time course as that of mt-cpYFP flashes (Figure S3), excluding the possibility that flashes reflect transient alkalinization of the mitochondrial matrix. Rather, several lines of evidence indicate that flashes reflect bursts of $O_2^{\cdot-}$ producing events, named “superoxide flashes”. First, application of MnTMPyP (50 μM), a SOD mimetic, decreases flash frequency by 83% and amplitude by 50% ($\Delta F/F_0 = 0.18 \pm 0.02$, n = 12; $p<0.01$ vs control; Figures 2C and 2D). Second, tiron (1 mM), a superoxide scavenger, similarly diminishes flash frequency and amplitude (Figures 2C and 2D), supporting the $O_2^{\cdot-}$ origin of mt-cpYFP flashes. Further, while mild uncoupling by 50 nM FCCP increases flavoprotein and decreases NADH autofluoresence due to their oxidation, it does not alter mt-cpYFP fluorescence (Figure S4). These results confirm that mt-cpYFP is not a nonspecific redox sensor. Finally, substituting the only two cysteine residues in mt-cpYFP with either alanine (C171A/C193A) or methionine (C171M/C193M) decreases basal probe fluorescence and renders the cysteine-free mt-cpYFP mutants insensitive to aldrithiol (Figure S5). Moreover, mitochondrial flash activity is not observed in cardiac cells expressing either mt-cpYFP double mutant (n = 15 cells), indicating that C171 and C193 contribute to a reactive center for $O_2^{\cdot-}$ sensing. Collectively, evidence presented thus far

demonstrates the presence of quantal events of mitochondrial $O_2^{\cdot-}$ production in cultured cardiomyocytes.

Superoxide flashes are not limited to cardiac cells, but are also observed in a wide range of cell types including neurons, neuroendocrine cells, skeletal myotubes, and non-excitable fibroblasts and osteosarcoma cells (Figures 2E–2I). Figure 2E illustrates representative superoxide flashes in spaghetti-shaped mitochondria recorded from primary cultured hippocampal neurons, indicating the reversibility of the flash-generating mechanism within individual mitochondria. Interestingly, superoxide flash frequency varies considerably between cell types. Flash frequency is 3.8 ± 0.5 (n = 53 cells) in adult cardiac myocytes, 31 ± 4 (n = 24 cells) in primary cultured hippocampal neurons, and 63 ± 6 (events per 1000 μm^2 cell area per 100 s, n = 37 cells) in PC12 pheochromocytoma cells (Figure 2F), suggesting cell type-specific regulation of quantal mitochondrial superoxide production. Despite variations in flash incidence and mitochondrial morphology among different cell types, superoxide flashes exhibit comparable properties (Figures 2G–2I), consistent with a common mechanism underlying superoxide flash genesis in all cells. Thus, real-time superoxide imaging uncovers intermittent, quantal bursts of $O_2^{\cdot-}$ production within the mitochondrial matrix of all cell types tested.

To confirm that mitochondrial superoxide flash activity is not an artifact of cell culture and viral transfection, we generated cardiac-specific mt-cpYFP transgenic mice (Figures 3A and 3B). Superoxide flashes of similar characteristics are detected in cardiac myocytes freshly isolated from these mice (Figure 3C). Furthermore, mitochondrial superoxide flash events are also visualized by high-resolution *ex vivo* imaging of mitochondria in the myocardium of intact, Langendorff-perfused and beating hearts (Figure 3D).

Molecular Mechanism of Superoxide Flash Initiation

We next explored the mechanism underlying mitochondrial superoxide flash genesis. Clues from superoxide flash characteristics are indicative of a sudden, all-or-none excitation of mitochondrial $O_2^{\cdot-}$-producing machinery. In isolated mitochondria, increased electron flow may cause dissipation of mitochondrial membrane potential ($\Delta\Psi_m$) and reduce ROS generation (Brand et al., 2004). However, recent evidence in intact cells indicates that brief openings of the mPTP by metabolic stress (Romashko et al., 1998), photostimulation (Zorov et al., 2000) and excessive ROS or Ca^{2+} (Duchen, 2000; Vercesi et al., 1997) result in transient depolarizations of m that stimulate ROS production (Huser et al., 1998) and solute exchange (<1,500 Da) between the mitochondrial matrix and cytosol (Bernardi, 1999; Crompton, 1999). While sustained mPTP activation is associated with cell injury and death due to its involvement in cytochrome c release and mitochondrial swelling (Crompton, 1999), several reports indicate that transient, sub-conductance mPTP openings also occur under physiological conditions (Ichas et al., 1997; Petronilli et al., 1999). Therefore, stochastic openings of the mPTP in quiescent cells may trigger superoxide flash genesis. To test this hypothesis, we labeled mt-cpYFP expressing myocytes with TMRM, a $\Delta\Psi_m$ indicator whose fluorescence signal is spectrally separable from that of mt-cpYFP (Figure 4A). Simultaneous measurement of TMRM and mt-cpYFP signals reveals that every superoxide flash coincides with a transient decrease in $\Delta\Psi_m$ (n = 89 events from 19 cells, a representative trace is shown in Figure 4B). On the other hand, not every transient depolarization is accompanied by a superoxide flash (n = 40 events from 5 cells, a representative trace is shown in Figure 4C). Further, superoxide flashes always coincide with a rapid and irreversible reduction in mitochondrial-entrapped rhod-2 fluorescence (752 Da, commonly used as a Ca^{2+} indicator, n = 8, Figure 4D), suggesting that a fraction of rhod-2 leaks out of the matrix through the mPTP during a superoxide flash.

If transient mPTP openings trigger superoxide flashes, then manipulation of mPTP activity should alter superoxide flash frequency. Indeed, bongkrekic acid (BA, 100 μM), an inhibitor

of the adenine nucleotide translocator that causes a conformation-dependent inhibition of the mPTP, attenuates the incidence of superoxide flashes to 33% of control while also decreasing their amplitude and abbreviating their kinetics (Figure 4E). Similar results are observed with cyclosporine A (1 μM, Figure 4E), a mPTP inhibitor that binds to cyclophilin D and also inhibits calcineurin (Bernardi, 1996; Montero et al., 2004). Conversely, mPTP activation by atractyloside (20 μM) significantly augments superoxide flash frequency (Figure 4E). Given significant limitations inherent in pharmacological manipulation of mPTP activity, we also determined the effect of RNA interference (siRNA) knockdown of cyclophilin D, a critical component of the mPTP (Baines et al., 2005; Basso et al., 2005; Nakagawa et al., 2005; Schinzel et al., 2005). Knockdown of cyclophilin D (70.0 ± 1.3% of control, n = 4, $p<0.05$, Figure 4F) by two sets of siRNA constructs causes a similar diminution in superoxide flash activity (75% of control, n = 53–57, $p<0.05$, Figure 4F). Taken together, we conclude that mPTP openings are both necessary and sufficient for triggering superoxide flashes in quiescent cells. In this regard, superoxide flash activity provides a powerful means for tracking transient mPTP activity in living cells.

The brief, highly localized and quantal nature of mitochondrial superoxide flash activity is analogous to another elementary intracellular signaling event - Ca^{2+} sparks, which arise from openings of an array of ryanodine receptor Ca^{2+} release channels in the endoplasmic and sarcoplasmic reticulum (Cheng et al., 1993). Previous studies have shown that mitochondria adjacent to local sites of Ca^{2+} release are able to sequester a fraction of the Ca^{2+} released during a Ca^{2+} spark (Ramesh et al., 1998). Since an increase in matrix Ca^{2+} activates the mPTP (Duchen, 2000), we explored the relationship between Ca^{2+} sparks and mitochondrial superoxide flashes. In adult cardiac myocytes, the frequency of spontaneous Ca^{2+} sparks outnumbers that of spontaneous superoxide flashes by two orders of magnitude (Figure S6). More importantly, superoxide flash frequency is unaltered by either a 2-fold increase (caffeine 1 mM) or an abolition of Ca^{2+} sparks (ryanodine and thapsigargin both at 10 μM for 15 min, Figure S6). These results exclude Ca^{2+} sparks as an obligatory trigger for superoxide flash production.

Mechanism of Superoxide Production during a Flash

We next determined the molecular mechanism of mPTP-mediated ROS generation. Previous studies have suggested that brief mPTP openings trigger massive electron leakage from the ETC due to altered membrane fluidity or rigidity (Mannella, 2006; Zorov et al., 2000) and conformational changes in proteins of the ETC (Batandier et al., 2004). Therefore, we hypothesize that ETC activity represents the source of mPTP-triggered superoxide flash production. To test this hypothesis, we used ρ° 143B TK^- human osteosarcoma cells that are devoid of mitochondrial DNA. In this cell model, mitochondrial respiration is abrogated altogether due to the absence of mitochondrial DNA-encoded ETC proteins (King and Attardi, 1989). In wild type 143B cells, robust superoxide flash activity is observed at a rate of 25 ± 4 events per 1000 μm^2 cell area per 100 s (n = 21 cells, Figures 5A and 5C). However, superoxide flashes are completely absent in ρ° cells (n = 20, Figures 5B and 5D) and are not revived by the mPTP activator atractyloside (Figures 5E and 5F). These results are consistent with superoxide flash production requiring ETC activity. We also created an ETC defective (ρ^-) cell model through inhibiting mitochondrial DNA replication in rat PC12 pheochromocytoma cells by incubation with EB (200 ng/ml) for up to 60 days (Biswas et al., 1999). EB-induced partial deprivation of mitochondrial DNA in ρ^- PC12 cells results in a parallel decrease in both cytochrome C oxidase subunit I (COX-1) expression (30% of control) and superoxide flash frequency (40% of control, from 63 ± 6 to 23 ± 3 events per 1000 μm^2 cell area per 100 s, n = 37–46 cells, Figure 5G). Finally, superoxide flash activity in cardiac myocytes and PC12 cells is abolished following blockade of electron flow at complex I, III and IV by rotenone (5 μM), antimycin A (5 μg/ml) or myxothiazol (5 μM) and sodium cyanide (5 mM), respectively

(Figures 5G and 5H), confirming the essential role of ETC activity for superoxide flash production (see Discussion). Finally, we also found that superoxide flash activity is abolished by complex V inhibitor, oligomycin (5 μM) and the H^+-ionophore, FCCP (300 nM) (Figure 5H), suggesting that ETC-coupled ATP synthesis is also required for superoxide flash genesis.

Alterations in Superoxide Flash Incidence during Cardiac Anoxia/Hypoxia-Reoxygenation

Reperfusion after ischemia, such as during myocardial infarction and ischemic stroke, is associated with a robust and destructive burst in ROS, whose subcellular and molecular origin remains undefined (Li and Jackson, 2002; Zweier et al., 1987). Therefore, we determined the incidence of mitochondrial superoxide flash activity in cardiac myocytes during anoxia/hypoxia and reoxygenation to test the hypothesis that increased mitochondrial superoxide flash activity contributes to the destructive ROS burst observed during early reperfusion.

Superoxide flash frequency is decreased by 60–70% in cardiac myocytes during either sustained anoxic treatment (95% N_2 and 5% CO_2 for 6 hrs, Figures 6A–C) or mild hypoxia (1% O_2 and 99% N_2 for 2 hrs, Figure 6D). These findings indicate that elevations in cytosolic levels of ROS during mild hypoxia (Guzy et al., 2005; Mansfield et al., 2005) most likely result from decreased ROS detoxification and/or increased extramitochondrial ROS production, but not increased superoxide flash activity. Following reoxygenation from 1% hypoxia, superoxide flash activity returns rapidly to normal levels during early reoxygenation (Figure 6D). More importantly, a rebound increase in superoxide flash activity (1.9-fold increase over control) is observed shortly after reoxygenation following anoxia (Figure 6C), a critical period of increased cell vulnerability to oxidative damage (Weiss et al., 2003). Superoxide flash activity then eventually recedes to a level below that of normoxia control (Figures 6C), consistent with irreversible mitochondrial damage inflicted during anoxia.

Previous studies have shown that damage associated with ischemia-reperfusion is alleviated by preconditioning cells with adenosine (Downey et al., 2007). Likewise, adenosine pretreatment (100 μM added 1 hr prior to anoxia) prevents the rebound flurry of superoxide flash activity observed during early reoxygenation following anoxia (Figure 6C), indicating that the cardioprotective effect of adenosine is associated with a suppression of increased superoxide flash production that otherwise occurs during reperfusion. These results not only support the idea of mitochondria as an important source of destructive ROS bursts during early reperfusion, but also demonstrate the utility of superoxide flashes as a quantitative biomarker for disorders characterized by increased oxidative stress.

DISCUSSION

The central and surprising finding of the present study is that individual mitochondria in quiescent cells display quantal bursts of superoxide production within the matrix, named superoxide flashes, under resting conditions. Single-mitochondrial superoxide flashes occur stochastically over space and time in living cells of diverse types, including cardiac myocytes, neurons and non-excitable cells. Mechanistically, superoxide flashes arise from a functional coupling between transient mPTP opening and ETC-dependent ROS production. Given their all-or-none appearance and single-mitochondrion confinement, we conclude that superoxide flashes constitute elementary events of quantal ROS generation within a single mitochondrion.

In order to interpret our findings in the context of previous published information, a key issue is that mPTP-triggered superoxide production may not be identical to “constitutive” ROS production from the ETC when the mPTP remains closed, as illustrated in our working hypothesis for mitochondrial superoxide flash production (Figure 7). In quiescence, a low-level of constitutive electron leak from the ETC raises matrix ROS to a level sufficient to trigger brief, stochastic openings of the mPTP, perhaps through reversible thiol oxidation (Petronilli

et al., 1994). Transient mPTP openings trigger ETC-mediated and ATP-dependent bursts in $O_2^{\cdot-}$ production, giving rise to a superoxide flash that coincides with transient dissipation of the inner membrane electrical gradient, matrix acidosis, mitochondrial swelling due to water movement, and altered structure and fluidity of the mitochondrial inner membrane. Spontaneous termination of the flash may be caused by matrix acidification that inhibits the mPTP through reversible protonation of histidyl residues (Nicolli et al., 1993).

Our results show that ETC blockade at any site as well as inhibition of the ATP synthase is sufficient to abolish superoxide flash activity. These findings indicate that fully intact ETC and ATP synthetic activities are required for superoxide flash genesis. Previous studies have suggested that ETC inhibition by rotenone either decreases (Aon et al., 2003; Chandel et al., 1998) or increases (Barrientos and Moraes, 1999; Chen et al., 2003; Nakamura et al., 2001; Turrens and Boveris, 1980) mitochondrial ROS production. Discrepancies also exist with regard to the effect of antimycin A and oligomycin on intracellular ROS levels. These findings underscore the notion that mPTP-triggered superoxide activity in the matrix and total cellular levels of ROS may be differentially regulated. Alternatively, discrepancies might also stem from the different probes (DCF versus mt-cpYFP) and experimental conditions (e.g., isolated mitochondrial versus intact cells) employed. Thus, resolution of mitochondrial matrix-restricted superoxide production with mt-cpYFP provides a novel means for potentially reconciling ongoing controversies that pervade the field of mitochondrial ROS signaling.

Because superoxide produced in the mitochondrial matrix can be readily converted to H_2O_2, a membrane-permeant and more stable ROS, our finding of discrete superoxide flash events provides a potential frequency-dependent mechanism for localized ROS signaling. By analogy to local control of Ca^{2+} signaling, we propose that individual superoxide flashes, once converted to long-lived and freely diffusible ROS derivatives, would create microdomains of high ROS concentration on a low global ROS background. Within these microdomains, transient high levels of ROS could activate high-threshold ROS signaling pathways (e.g., activation/inactivation of kinases, phosphatases, channels or transporters) that remain dormant elsewhere in the cell where global ROS concentrations remain low. Downstream ROS scavenging enzymes and small molecules (e.g. peroxidases, catalase, glutathione, glutathione reductase, mitochondrial NADPH-producing enzymes and thioredoxins) will also impact local ROS signaling initiated by superoxide flash activity. At the whole cell level, spatiotemporal summation of ROS microdomains could provide a mechanism for diversification of ROS signaling in accordance with superoxide flash frequency. Future work is clearly required in order to determine the degree to which quantal mitochondrial superoxide production contributes to local and global ROS signaling.

It is well-established that mPTP plays a critical role in stress-related ROS signaling, mitochondrial dysfunction and apoptotic cell death (Baines et al., 2005; Crompton, 1999; Nakagawa et al., 2005). However, tracking mPTP activity in individual mitochondria of intact cells has been a major challenge. In the present study, we demonstrate the use of superoxide flashes as an optical readout of mPTP activity in living cells. The reversible and sometimes repetitive nature of superoxide flash activity across diverse cell types as well as in the beating heart strongly indicates that mPTP functions within a physiological context. We anticipate that *in situ* monitoring of mPTP function through superoxide flash activity in conjunction with genetic manipulation of putative mPTP components (e.g. cyclophilin D) will greatly advance our knowledge of the molecular identity of mPTP and its biological function in health and disease.

Our results also provide novel insight into the pathophysiological mechanisms of oxidative stress-related disorders and potential therapeutic targets for intervention. Increased oxidation or ROS bursts are implicated in hypoxia/reoxygenation injury and other stress perturbations

including metabolic inhibition (Romashko et al., 1998) and proapoptotic stimulation (Chandra et al., 2000). Our results provide direct evidence for how pathological mPTP activation is coupled to uncontrolled ROS production that results in deleterious effects on cell function. The apparent discrepancy between a decrease in superoxide flash activity within the mitochondrial matrix (our data) and increase in whole cell levels of ROS during hypoxia (Guzy et al., 2005; Mansfield et al., 2005) can be reconciled: a decrease in the probability of mPTP opening due to cytosolic acidosis, elevated Mg^{2+} and depressed electron transport (Griffiths and Halestrap, 1995; Honda et al., 2005) would reduce superoxide flash activity in the mitochondrial matrix, whereas a severely inhibited antioxidant (ROS detoxification) system and an imbalance between mitochondrial and cytosolic ROS production during hypoxia/anoxia could result in a net increase in global levels of ROS. Taken together, we propose that superoxide flash activity can be used as a biomarker for mPTP- and oxidative stress-related pathologies. Moreover, our finding that superoxide flash activity is inhibited by interventions that reduce mPTP activation (e.g. exposure to BA, cyclosporine A or adenosine and cyclophilin D knockdown) reinforces the notion that the mPTP represents an intriguing potential therapeutic target to combat irreversible damage following ischemia/reperfusion.

In summary, the three major contributions of this study include: (1) the discovery of quantal and transient superoxide-producing events within single mitochondria across multiple cell types and within the intact heart under resting conditions, (2) the demonstration that mitochondrial superoxide flash biogenesis involves a unique functional coupling between transient mPTP opening and increased superoxide generation via the ETC- and ATP-dependent pathways, and (3) the observation that an increased flurry of mitochondrial superoxide flash activity contributes to the destructive burst of ROS produced during reoxygenation following a period of anoxia. These advances are built upon the development and characterization of a highly sensitive and reversible superoxide-selective probe, a circularly permutated yellow fluorescent protein bearing Cys171 and Cys193 residues that form a reactive superoxide sensor. Just as Ca^{2+} sparks represent elementary units of Ca^{2+}-induced Ca^{2+} release gated by intracellular Ca^{2+} release channels, mitochondrial superoxide flashes constitute elemental all-or-none events of quantal mitochondrial ROS production triggered by the mPTP. As such, superoxide flashes open a unique vista for investigations of ROS signaling, ETC activity and mPTP regulation in single mitochondria and may also serve as a valuable biomarker for oxidative stress-related diseases.

EXPERIMENTAL PROCEDURES

Spectral Analysis of cpYFP

cpYFP cDNA (807 bp) was cloned into pRSET and transferred into *E. coli.* (BL21(DE3)LysS) for large-scale protein expression. *In vitro* redox calibration of cpYFP fluorescence was carried out using methods described previously (Hanson et al., 2004). Emission and excitation spectra of reduced and oxidized cpYFP in the presence of designated reagents were obtained with a spectrofluorimeter (Model: CM1T10I, HORIBA Jobin Yvon, Inc.) continuously purged with nitrogen gas.

Confocal Imaging

Enzymatically isolated rat ventricular myocytes and hippocampal neurons in primary culture were infected with adenovirus carrying the mt-cpYFP coding sequence or its mutants at an m.o.i. of 100 and cultured for 2 to 3 days. Similar conditions were used when expressing mt-cpYFP in other cell types. Confocal imaging used a Zeiss LSM 510 confocal microscope equipped with a 63x, 1.3NA oil immersion objective and a sampling rate of 0.7 s/frame. Dual excitation imaging of mt-cpYFP was achieved by alternating excitation at 405 and 488 nm and collecting emission at >505 nm. Tri-wavelength excitation imaging of mt-cpYFP and TMRM

(20 nM) or rhod-2 was achieved by tandem excitation at 405, 488, and 543 nm, and the emission was collected at 515–550, 515–550 and >560 nm, respectively. To obtain optimized mitochondrial retention of rhod-2, we adopted the protocol of Hajnoczky et al. (1995) with modification. Flavoprotein (FAD) fluorescence emission was measured at >505 nm with excitation at 458 nm. NADH autofluorescence was excited at 365 nm and measured over 420–470 nm. Imaging experiments were performed at room temperature (22–26°C). Digital image processing used the IDL software (Research Systems) and customer-devised programs.

For in vivo imaging of single mitochondrial superoxide flash activity, Langendorff-perfused hearts from transgenic mice with cardiac-specific expression of mt-cpYFP were placed on the stage of a confocal microscope and perfused with Tyrode's solution. The fluorescence acquisition plane was focused ~30 μm into the myocardium from the heart surface. Motion artifacts due to the heartbeat (480/min) were minimized by a myofilament inhibitor, blebbistatin (10 μM). Recordings were carried out at 35°C.

Mitochondrial DNA-Deleted or Deficient (ρ° or ρ⁻) Cells

ρ° 143B TK⁻ human osteosarcoma cells and its wild type control were a kind gift from Dr. Nadja C. de Souza-Pinto (National Institute on Aging, NIH). ρ° 143B cells lack mitochondrial respiration due to loss of critical ETC proteins encoded by mitochondrial DNA. To partially deplete mitochondrial DNA and allow partial disruption of mitochondrial respiration, PC12 pheochromocytoma cells were cultured in the presence of 200 ng/ml ethidium bromide, 100 μg/ml pyruvate and 50 μg/ml uridine for up to 60 days. Depletion of mitochondrial DNA was confirmed by western blot analysis of cytochrome C oxidase subunit I.

Anoxia, Hypoxia and Reoxygenation Treatment of Cardiac Myocytes

For anoxia, cardiomyocytes expressing mt-cpYFP were cultured in an anoxia chamber (Billups-Rothenberg) at 37°C and ventilated with 95% N_2 plus 5% CO_2 for 6 hours. At the end of anoxia treatment, culture dishes were sealed with a plastic cover and immediately transferred onto the stage of a confocal microscope. For hypoxia, cells were cultured in a sealed chamber on the confocal stage and perfused with hypoxia solution (saturated with 1% O_2 + 99% N_2) at room temperature. After recording superoxide flashes under anoxic/hypoxic conditions, reoxygenation was achieved by removing the seal and superfusing cells with oxygenated extracellular solution.

Statistics

Data are reported as mean ± SEM. Paired and unpaired Student's *t* test and ANOVA with repeated measurements were applied, when appropriate, to determine statistical significance of the differences. $P<0.05$ was considered statistically significant.

Supplementary Material

Refer to Web version on PubMed Central for supplementary material.

ACKNOWLEDGEMENTS

We thank Drs. R. P. Xiao, X. L. Tian, W. J. Lederer, and S. J. Sollott for helpful discussions and critical comments, and D. Yang, H. A. Spurgeon, B. D. Ziman, and Y. Wang for technical supports. W. Wang and H.Q. Fang are co-first authors. This work was supported by the NIH intramural (W.W., E.G.L., H.C., M.P.M.) and extramural Research Program (J.P.K., R.T.D. (AR44657), S.S.S. (HL-33333)), Chinese National Natural Science Foundation (H.C., J.L.) and Major State Basic Research Development Programs of China (2007CB512100).

REFERENCES

Andersen JK. Oxidative stress in neurodegeneration: cause or consequence? Nat Med 2004;10:S18–S25. [PubMed: 15298006]

Aon MA, Cortassa S, Marban E, O'Rourke B. Synchronized whole cell oscillations in mitochondrial metabolism triggered by a local release of reactive oxygen species in cardiac myocytes. J Biol Chem 2003;278:44735–44744. [PubMed: 12930841]

Baines CP, Kaiser RA, Purcell NH, Blair NS, Osinska H, Hambleton MA, Brunskill EW, Sayen MR, Gottlieb RA, Dorn GW, et al. Loss of cyclophilin D reveals a critical role for mitochondrial permeability transition in cell death. Nature 2005;434:658–662. [PubMed: 15800627]

Barrientos A, Moraes CT. Titrating the effects of mitochondrial complex I impairment in the cell physiology. J Biol Chem 1999;274:16188–16197. [PubMed: 10347173]

Basso E, Fante L, Fowlkes J, Petronilli V, Forte MA, Bernardi P. Properties of the permeability transition pore in mitochondria devoid of Cyclophilin D. J Biol Chem 2005;280:18558–18561. [PubMed: 15792954]

Batandier C, Leverve X, Fontaine E. Opening of the mitochondrial permeability transition pore induces reactive oxygen species production at the level of the respiratory chain complex I. J Biol Chem 2004;279:17197–17204. [PubMed: 14963044]

Beckman KB, Ames BN. The free radical theory of aging matures. Physiol Rev 1998;78:547–581. [PubMed: 9562038]

Belousov VV, Fradkov AF, Lukyanov KA, Staroverov DB, Shakhbazov KS, Terskikh AV, Lukyanov S. Genetically encoded fluorescent indicator for intracellular hydrogen peroxide. Nat Methods 2006;3:281–286. [PubMed: 16554833]

Bernardi P. The permeability transition pore. Control points of a cyclosporin A-sensitive mitochondrial channel involved in cell death. Biochim Biophys Acta 1996;1275:5–9. [PubMed: 8688451]

Bernardi P. Mitochondrial Transport of Cations: Channels, Exchangers, and Permeability Transition. Physiol Rev 1999;79:1127–1155. [PubMed: 10508231]

Biswas G, Adebanjo OA, Freedman BD, Anandatheerthavarada HK, Vijayasarathy C, Zaidi M, Kotlikoff M, Avadhani NG. Retrograde Ca^{2+} signaling in C2C12 skeletal myocytes in response to mitochondrial genetic and metabolic stress: a novel mode of inter-organelle crosstalk. EMBO J 1999;18:522–533. [PubMed: 9927412]

Brand MD, Affourtit C, Esteves TC, Green K, Lambert AJ, Miwa S, Pakay JL, Parker N. Mitochondrial superoxide: production, biological effects, and activation of uncoupling proteins. Free Radic Biol Med 2004;37:755–767. [PubMed: 15304252]

Brookes PS, Yoon Y, Robotham JL, Anders MW, Sheu SS. Calcium, ATP, and ROS: a mitochondrial love-hate triangle. Am J Physiol Cell Physiol 2004;287:C817–C833. [PubMed: 15355853]

Chandel NS, Maltepe E, Goldwasser E, Mathieu CE, Simon MC, Schumacker PT. Mitochondrial reactive oxygen species trigger hypoxia-induced transcription. Proc Natl Acad Sci U S A 1998;95:11715–11720. [PubMed: 9751731]

Chandra J, Samali A, Orrenius S. Triggering and modulation of apoptosis by oxidative stress. Free Radic Biol Med 2000;29:323–333. [PubMed: 11035261]

Chen Q, Vazquez EJ, Moghaddas S, Hoppel CL, Lesnefsky EJ. Production of reactive oxygen species by mitochondria: central role of complex III. J Biol Chem 2003;278:36027–36031. [PubMed: 12840017]

Cheng H, Lederer WJ, Cannell MB. Calcium sparks: elementary events underlying excitation-contraction coupling in heart muscle. Science 1993;262:740–744. [PubMed: 8235594]

Crompton M. The mitochondrial permeability transition pore and its role in cell death. Biochem J 1999;341:233–249. [PubMed: 10393078]

Dhalla NS, Temsah RM, Netticadan T. Role of oxidative stress in cardiovascular diseases. J Hypertens 2000;18:655–673. [PubMed: 10872549]

Downey JM, Davis AM, Cohen MV. Signaling pathways in ischemic preconditioning. Heart Fail Rev 2007;12:181–188. [PubMed: 17516169]

Droege W. Free radicals in the physiological control of cell function. Physiol Rev 2002;82:47–95. [PubMed: 11773609]

Duchen MR. Mitochondria and Ca^{2+} in cell physiology and pathophysiology. Cell Calcium 2000;28:339–348. [PubMed: 11115373]

Dypbukt JM, Ankarcrona M, Burkitt M, Sjoholm A, Strom K, Orrenius S, Nicotera P. Different prooxidant levels stimulate growth, trigger apoptosis, or produce necrosis of insulin-secreting RINm5F cells. The role of intracellular polyamines. J Biol Chem 1994;269:30553–30560. [PubMed: 7982974]

Griffiths EJ, Halestrap AP. Mitochondrial non-specific pores remain closed during cardiac ischaemia, but open upon reperfusion. Biochem J 1995;307:93–98. [PubMed: 7717999]

Guzy RD, Hoyos B, Robin E, Chen H, Liu L, Mansfield KD, Simon MC, Hammerling U, Schumacker PT. Mitochondrial complex III is required for hypoxia-induced ROS production and cellular oxygen sensing. Cell Metab 2005;1:401–408. [PubMed: 16054089]

Hanson GT, Aggeler R, Oglesbee D, Cannon M, Capaldi RA, Tsien RY, Remington SJ. Investigating mitochondrial redox potential with redox-sensitive green fluorescent protein indicators. J Biol Chem 2004;279:13044–13053. [PubMed: 14722062]

Honda HM, Korge P, Weiss JN. Mitochondria and ischemia/reperfusion injury. Ann N Y Acad Sci 2005;1047:248–258. [PubMed: 16093501]

Huser J, Rechenmacher CE, Blatter LA. Imaging the permeability pore transition in single mitochondria. Biophys J 1998;74:2129–2137. [PubMed: 9545072]

Ichas F, Jouaville LS, Mazat JP. Mitochondria are excitable organelles capable of generating and conveying electrical and calcium signals. Cell 1997;89:1145–1153. [PubMed: 9215636]

Isaeva EV, Shkryl VM, Shirokova N. Mitochondrial redox state and Ca^{2+} sparks in permeabilized mammalian skeletal muscle. J Physiol 2005;565:855–872. [PubMed: 15845582]

King MP, Attardi G. Human cells lacking mtDNA: repopulation with exogenous mitochondria by complementation. Science 1989;246:500–503. [PubMed: 2814477]

Klaunig JE, Kamendulis LM. The role of oxidative stress in carcinogenesis. Annu Rev Pharmacol Toxicol 2004;44:239–267. [PubMed: 14744246]

Li C, Jackson RM. Reactive species mechanisms of cellular hypoxia-reoxygenation injury. Am J Physiol Cell Physiol 2002;282:C227–C241. [PubMed: 11788333]

Mannella CA. Structure and dynamics of the mitochondrial inner membrane cristae. Biochim Biophys Acta 2006;1763:542–548. [PubMed: 16730811]

Mansfield KD, Guzy RD, Pan Y, Young RM, Cash TP, Schumacker PT, Simon MC. Mitochondrial dysfunction resulting from loss of cytochrome c impairs cellular oxygen sensing and hypoxic HIF-α activation. Cell Metab 2005;1:393–399. [PubMed: 16054088]

Montero M, Lobaton CD, Gutierrez-Fernandez S, Moreno A, Alvarez J. Calcineurin-independent inhibition of mitochondrial Ca^{2+} uptake by cyclosporin A. Br J Pharmacol 2004;141:263–268. [PubMed: 14691054]

Nagai T, Sawano A, Park ES, Miyawaki A. Circularly permuted green fluorescent proteins engineered to sense Ca^{2+} Proc Natl Acad Sci U S A 2001;98:3197–3202. [PubMed: 11248055]

Nakagawa T, Shimizu S, Watanabe T, Yamaguchi O, Otsu K, Yamagata H, Inohara H, Kubo T, Tsujimoto Y. Cyclophilin D-dependent mitochondrial permeability transition regulates some necrotic but not apoptotic cell death. Nature 2005;434:652–658. [PubMed: 15800626]

Nakamura K, Bindokas VP, Kowlessur D, Elas M, Milstien S, Marks JD, Halpern HJ, Kang UJ. Tetrahydrobiopterin scavenges superoxide in dopaminergic neurons. J Biol Chem 2001;276:34402–34407. [PubMed: 11447224]

Nicolli A, Petronilli V, Bernardi P. Modulation of the mitochondrial cyclosporin A-sensitive permeability transition pore by matrix pH. Evidence that the pore open-closed probability is regulated by reversible histidine protonation. Biochemistry 1993;32:4461–4465. [PubMed: 7682848]

Ostergaard H, Henriksen A, Hansen FG, Winther JR. Shedding light on disulfide bond formation: engineering a redox switch in green fluorescent protein. EMBO J 2001;20:5853–5862. [PubMed: 11689426]

Otani H. Reactive oxygen species as mediators of signal transduction in ischemic preconditioning. Antioxid Redox Signal 2004;6:449–469. [PubMed: 15025947]

Petronilli V, Costantini P, Scorrano L, Colonna R, Passamonti S, Bernardi P. The voltage sensor of the mitochondrial permeability transition pore is tuned by the oxidation-reduction state of vicinal thiols.

Increase of the gating potential by oxidants and its reversal by reducing agents. J Biol Chem 1994;269:16638–16642. [PubMed: 7515881]

Petronilli V, Miotto G, Canton M, Brini M, Colonna R, Bernardi P, Di Lisa F. Transient and long-lasting openings of the mitochondrial permeability transition pore can be monitored directly in intact cells by changes in mitochondrial calcein fluorescence. Biophys J 1999;76:725–734. [PubMed: 9929477]

Ramesh V, Sharma VK, Sheu SS, Franzini-Armstrong C. Structural proximity of mitochondria to calcium release units in rat ventricular myocardium may suggest a role in Ca^{2+} sequestration. Ann N Y Acad Sci 1998;853:341–344. [PubMed: 10603975]

Romashko DN, Marban E, O'Rourke B. Subcellular metabolic transients and mitochondrial redox waves in heart cells. Proc Natl Acad Sci U S A 1998;95:1618–1623. [PubMed: 9465065]

Schinzel AC, Takeuchi O, Huang Z, Fisher JK, Zhou Z, Rubens J, Hetz C, Danial NN, Moskowitz MA, Korsmeyer SJ. Cyclophilin D is a component of mitochondrial permeability transition and mediates neuronal cell death after focal cerebral ischemia. Proc Natl Acad Sci U S A 2005;102:12005–12010. [PubMed: 16103352]

Takahashi A, Zhang Y, Centonze E, Herman B. Measurement of mitochondrial pH in situ. Biotechniques 2001;30:804–808. [PubMed: 11314264]810, 812 passim

Turrens JF, Boveris A. Generation of superoxide anion by the NADH dehydrogenase of bovine heart mitochondria. Biochem J 1980;191:421–427. [PubMed: 6263247]

Vercesi AE, Kowaltowski AJ, Grijalba MT, Meinicke AR, Castilho RF. The role of reactive oxygen species in mitochondrial permeability transition. Biosci Rep 1997;17:43–52. [PubMed: 9171920]

Wallace DC. A mitochondrial paradigm for degenerative diseases and ageing. Novartis Found Symp 2001a;235:247–263. [PubMed: 11280029]

Wallace DC. A mitochondrial paradigm for degenerative diseases and ageing. Novartis Found Symp 2001b;235:247–263. [PubMed: 11280029]discussion 263-246

Weiss JN, Korge P, Honda HM, Ping P. Role of the mitochondrial permeability transition in myocardial disease. Circ Res 2003;93:292–301. [PubMed: 12933700]

Yan Y, Liu J, Wei C, Li K, Xie W, Wang Y, Cheng H. Bidirectional regulation of Ca^{2+} sparks by mitochondria-derived reactive oxygen species in cardiac myocytes. Cardiovasc Res 2008;77:432–441. [PubMed: 18006452]

Zima AV, Blatter LA. Redox regulation of cardiac calcium channels and transporters. Cardiovasc Res 2006;71:310–321. [PubMed: 16581043]

Zorov DB, Filburn CR, Klotz LO, Zweier JL, Sollott SJ. Reactive oxygen species ROS-induced ROS release: a new phenomenon accompanying induction of the mitochondrial permeability transition in cardiac myocytes. J Exp Med 2000;192:1001–1014. [PubMed: 11015441]

Zweier JL, Flaherty JT, Weisfeldt ML. Direct measurement of free radical generation following reperfusion of ischemic myocardium. Proc Natl Acad Sci U S A 1987;84:1404–1407. [PubMed: 3029779]

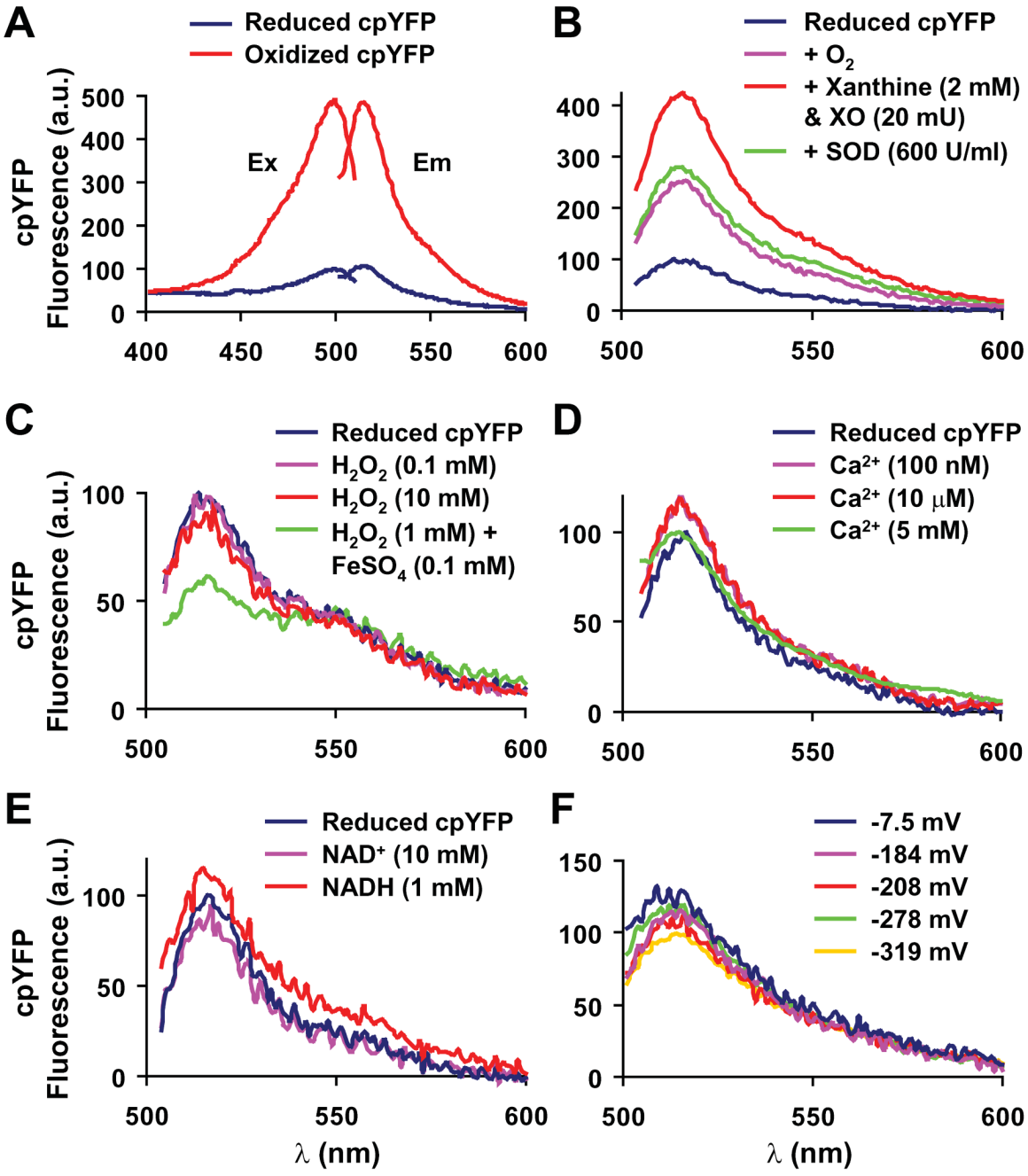

Figure 1. Circularly Permuted Yellow Fluorescent Protein (cpYFP) as a Superoxide Indicator

(A) Excitation and emission spectra for fully reduced (blue lines, 10 mM reduced DTT) and fully oxidized (red lines, 1 mM aldrithiol) cpYFP. Ex: Excitation spectra obtained at 515 nm emission; Em: Emission spectra at 488 nm excitation. An isosbestic point was identified near 405 nm excitation, permitting ratiometric measurement via dual wavelength excitation (488 nm/405 nm). (B) The increase of cpYFP fluorescence emission (at 488 nm excitation) when reduced cpYFP was exposed to xanthine (2 mM) plus xanthine oxidase (20 mU) under aerobic conditions and its complete reversal to the aerobic control level by subsequent addition of Cu/Zn-SOD (600 U/ml). (C) cpYFP emission was insensitive to H_2O_2 (0.1 and 10 mM) and slightly decreased by hydroxyl radical (produced by the Fenton reaction: 1 mM H_2O_2 plus 0.1 mM

$FeSO_4$ under anaerobic conditions). (D) cpYFP emission was insensitive to physiological concentrations of Ca^{2+}. (E) cpYFP emission was insensitive to NAD^+ (10 mM) and NADH (1 mM). (F) cpYFP emission was insensitive to a broad range of redox potentials (−7.5 ~ −319 mV). Solutions of variable redox potentials were made by mixing reduced and oxidized DTT in different proportions (total DTT concentration 10 mM). The exact redox potential for each mixture was monitored by a redox sensitive electrode (Orion 91-80, Thermo Electron) at pH 8.0 and 20–23°C. The same solutions were then used for cpYFP spectral measurement.

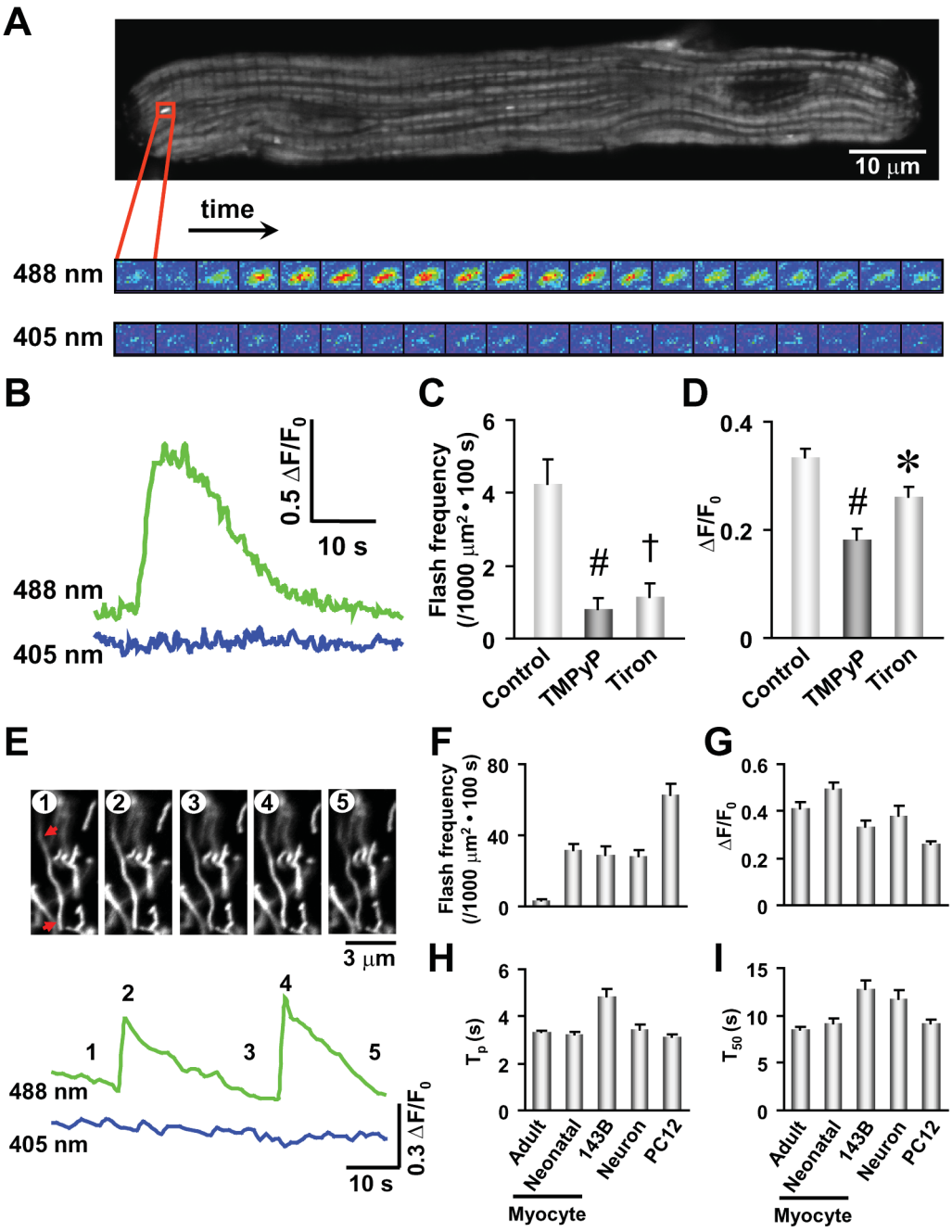

Figure 2. Superoxide Flashes in Single Mitochondria

(A) Confocal visualization of a single-mitochondrion superoxide flash in a rat cardiac myocyte. Upper panel: Confocal image of a cardiac myocyte expressing mt-cpYFP. The enlarged view shows dual excitation (488 and 405 nm) imaging of the superoxide flash at 2 s intervals. The area shown has dimensions of 2.2×1.7 μm^2. (B) Time course of the superoxide flash shown in A. (C and D) Depression of superoxide flash frequency (C) and amplitude ($\Delta F/F_0$, D) by an SOD mimetic, MnTMPyP (50 μM), and a superoxide scavenger, tiron (1 mM). Data are mean ± SEM. n = 12–64 flashes from 10–16 cells. *, $P<0.05$; #, $P<0.01$; †, $P<0.001$ versus control. (E) Superoxide flashes in primary cultured hippocampal neurons. Arrows mark two ends of a spaghetti-shaped mitochondrion undergoing repetitive superoxide flashes. Images correspond

to the designated time points (1–5). (F–I) Properties of superoxide flashes in different cell types. Frequency (F), amplitude ($\Delta F/F_0$, where F_0 refers to basal fluorescence intensity, G), time to peak (T_p, H), and 50% decay time after the peak (T_{50}, I). Data are mean ± SEM. n = 57–409 events from 21–53 cells.

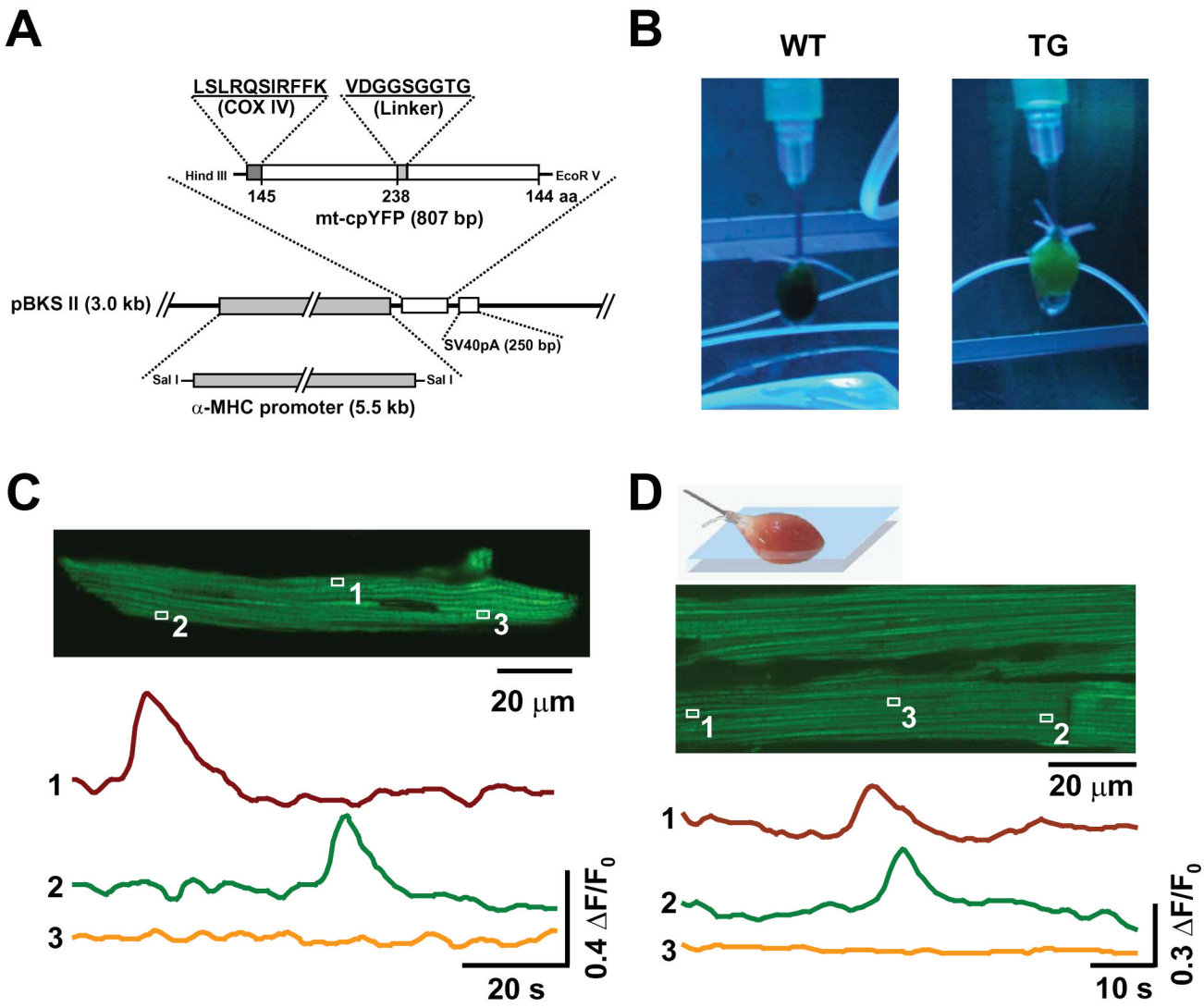

Figure 3. Superoxide Flashes in mt-cpYFP Transgenic Mice

(A) Schematic of the cardiac-specific mt-cpYFP expressing vector used to generate mt-cpYFP transgenic mice. (B) Images of Langendorff-perfused hearts of wild type (WT) and mt-cpYFP transgenic mice (TG) under UV illumination. Note the green fluorescence of the TG heart. (C) Visualization of superoxide flashes in a freshly isolated ventricular myocyte from a TG mouse. Upper panel: Image of a representative myocyte. Lower panel: Time course of the mt-cpYFP signals (488 nm excitation) from mitochondria indicated in the image, showing two active and one quiescent mitochondria. Similar results were obtained in 12 myocytes from 3 TG mice. (D) Imaging of superoxide flashes in the Langendorff-perfused heart from a TG mouse. Upper panel: Illustration of experimental setting. Middle panel: 2-D image of cardiac myocytes in the myocardium of the beating heart from a TG mouse. Lower panel: time course of mt-cpYFP signals from two active and one quiescent mitochondria (box 3, illustrating absence of motion artifact). Similar results were obtained in 4 other hearts.

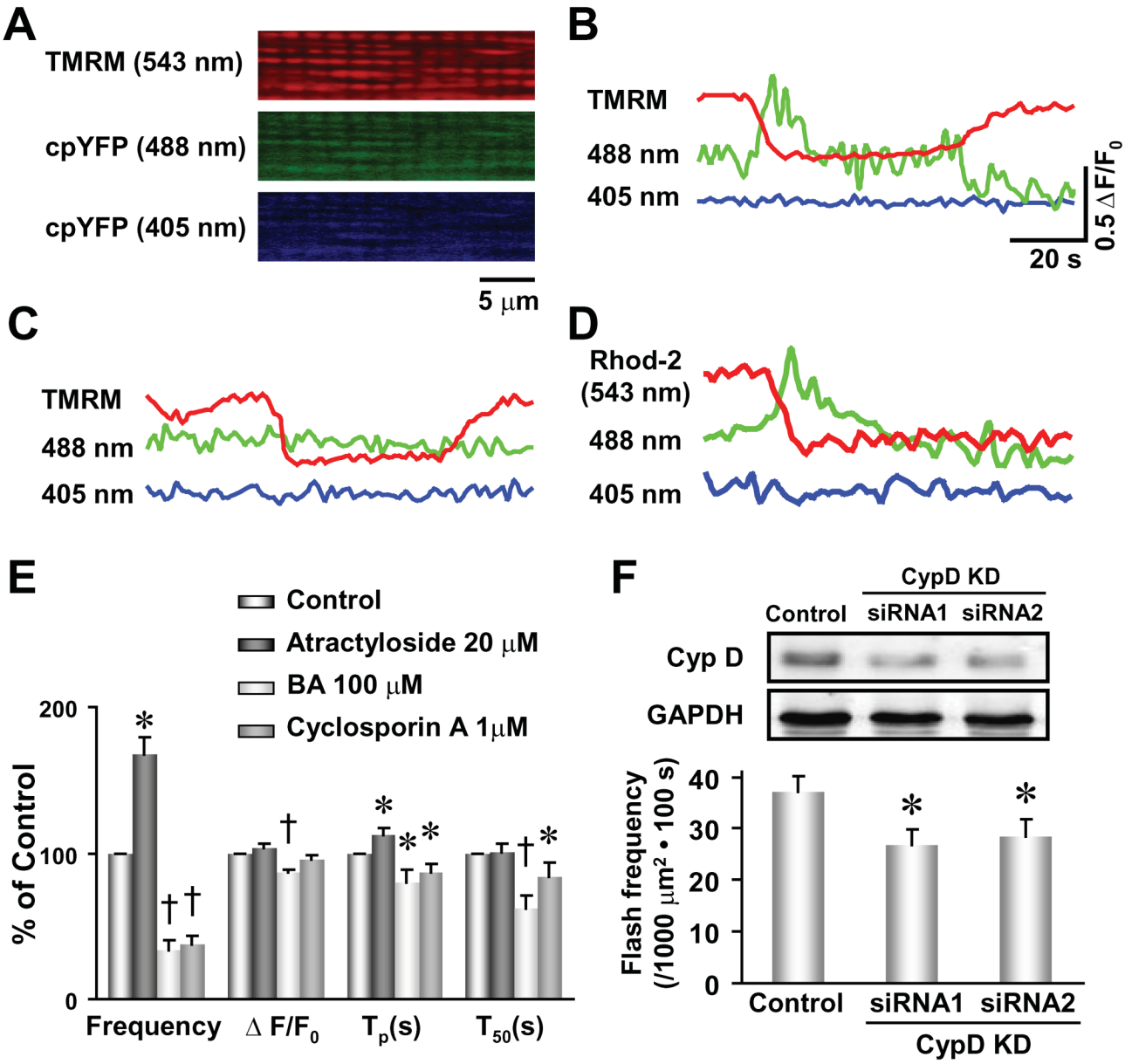

Figure 4. Opening of mPTP Triggers Superoxide Flash Activity

(A) Colocalization of the $\Delta\Psi_m$ indicator TMRM and the superoxide indicator mt-cpYFP in cardiac mitochondria revealed by tri-wavelength excitation imaging. (B and C) Two types of $\Delta\Psi_m$ depolarization were distinguished by the presence and absence of concurrent superoxide flashes. n = 83 events from 19 cells. (D) Permanent reduction in mitochondrial rhod-2 fluorescence coincides with the onset of a superoxide flash (n = 39 events in 8 cells). Scale bars in (B) apply to (B)–(D). (E) Opposing effects of mPTP activation by atractyloside (20 μM, n = 5 cells) and inhibition by either bongkrekic acid (BA, 100 μM, n = 16 cells) or cyclosporin A (1 μM, n = 15 cells) on superoxide flash properties. T_p, time to peak; T_{50}, time from peak to 50% decay. Data are mean ± SEM. *, $P<0.05$; †, $P<0.001$ versus control. (F) Knockdown of cyclophilin D (insert, CypD KD, n = 4) by two sets of siRNA constructs (siRNA1 and siRNA2) both significantly decreased superoxide flash incidence in neonatal cardiac myocytes. n = 53–57 cells. Data are mean ± SEM. *, $P<0.05$ versus control.

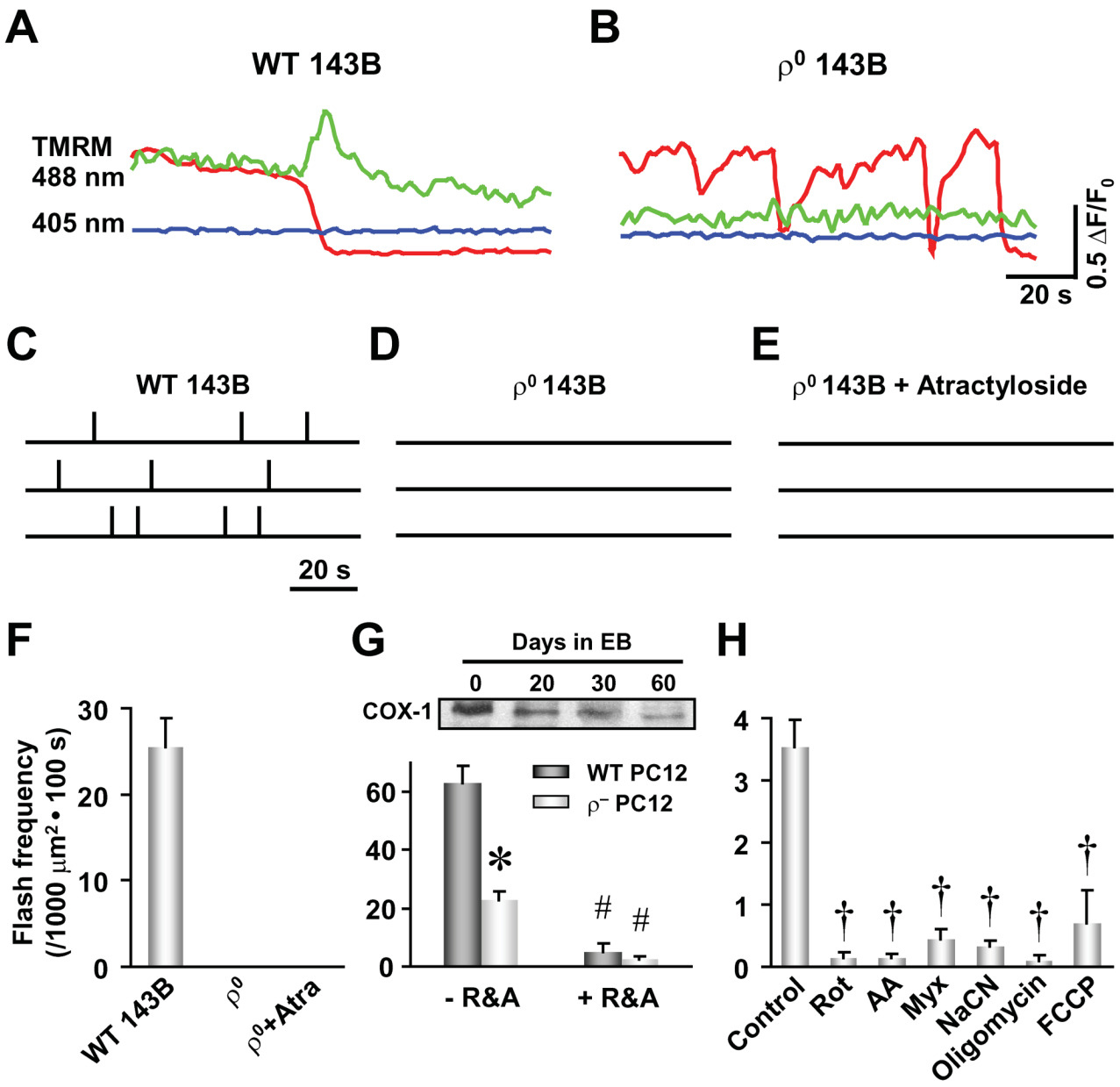

Figure 5. Role of Mitochondrial ETC Activity on Superoxide Flash Production

(A–F), Absence of superoxide flashes in 143B cells completely devoid of mitochondrial DNA (ρ° 143B). Superoxide flashes exhibiting a reduction in TMRM fluorescence were readily observed in wild type 143B TK⁻ human osteosarcoma cells (WT 143B) as shown by fluorescence traces (A) and three representative diaries of superoxide flash incidence (each vertical tick denotes a flash event, C), but not in ρ° 143B cells (B and D) in spite of the presence of $\Delta\Psi_m$ fluctuations (B). Atractyloside (Atra, 20 μM) did not rescue superoxide flash activity in ρ° 143B cells (E). Scale bars in (B) also apply to (A). (F) Statistics of superoxide flash frequency in WT and ρ° 143B cells. Data are mean ± SEM. n = 5–21 cells. (G) Attenuated superoxide flash activity in ETC-deficient cells. Upper panel: Inhibition of mitochondrial DNA replication by treatment of PC12 cells with ethidium bromide (EB, 200 ng/ml) for up to 60 days (referred to as ρ⁻ PC12 cells) resulted in a time-dependent decrease in the expression of the mitochondrial DNA-encoded cytochrome C oxidase subunit I (COX-1). Lower panel: a

significant decrease in the frequency of superoxide flashes was observed in ρ^- PC12 cells. R&A: rotenone (5 μM) and antimycin A (5 μg/ml). Data are mean ± SEM. n = 16–46 cells. *, $P<0.05$ versus wild type (WT PC12) cells. #, $P<0.01$ versus –R&A. (H) Inhibition of superoxide flash activity in rat adult cardiac myocytes by rotenone (Rot, 5 μM), antimycin A (AA, 5 μg/ml), myxothiazol (Myx, 5 μM), sodium cyanide (CN, 5 mM), oligomycin (5 μM), and FCCP (300 nM). Data are mean ± SEM. n = 7–18 cells. †, $P<0.001$ versus control. Label of Y axis in (F) applies to (F)–(H).

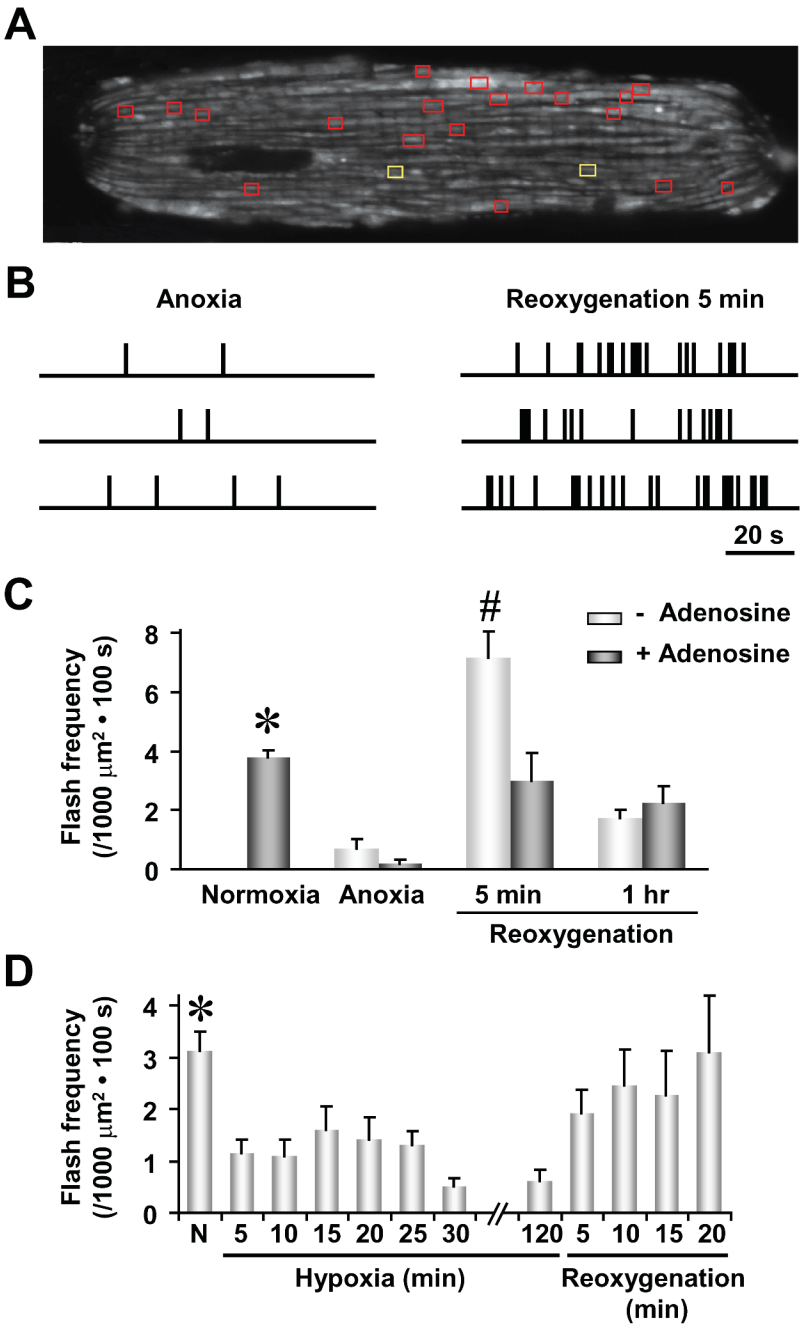

Figure 6. Superoxide Flash Production during Anoxia/Hypoxia and Reoxygenation

(A) Two-dimensional map of superoxide flashes in a cardiac cell. Yellow boxes mark locations of superoxide flashes detected during a 100 s-scan after 6 hr of anoxia and red boxes mark active sites ~5 min following reoxygenation. (B) Temporal diaries of superoxide flash incidence in three representative cells during anoxia (left panel) and reoxygenation (right panel). Data in the top rows correspond to the cell depicted in (A). (C) Averaged superoxide flash frequency during anoxia, 5 min after reoxygenation and 1 hr after reoxygenation, in the absence or presence of adenosine (100 μM, added 1 hr prior to anoxia). Data are mean ± SEM. n = 6–16 cells. *, $P<0.05$ versus all other groups; #, $P<0.01$ versus adenosine. (D) Time course

of superoxide flash frequency during hypoxia (1% O_2 + 99% N_2) and early reoxygenation. Data are mean ± SEM. n = 10–51 cells. *, $P<0.05$ normoxia (N) versus hypoxia.

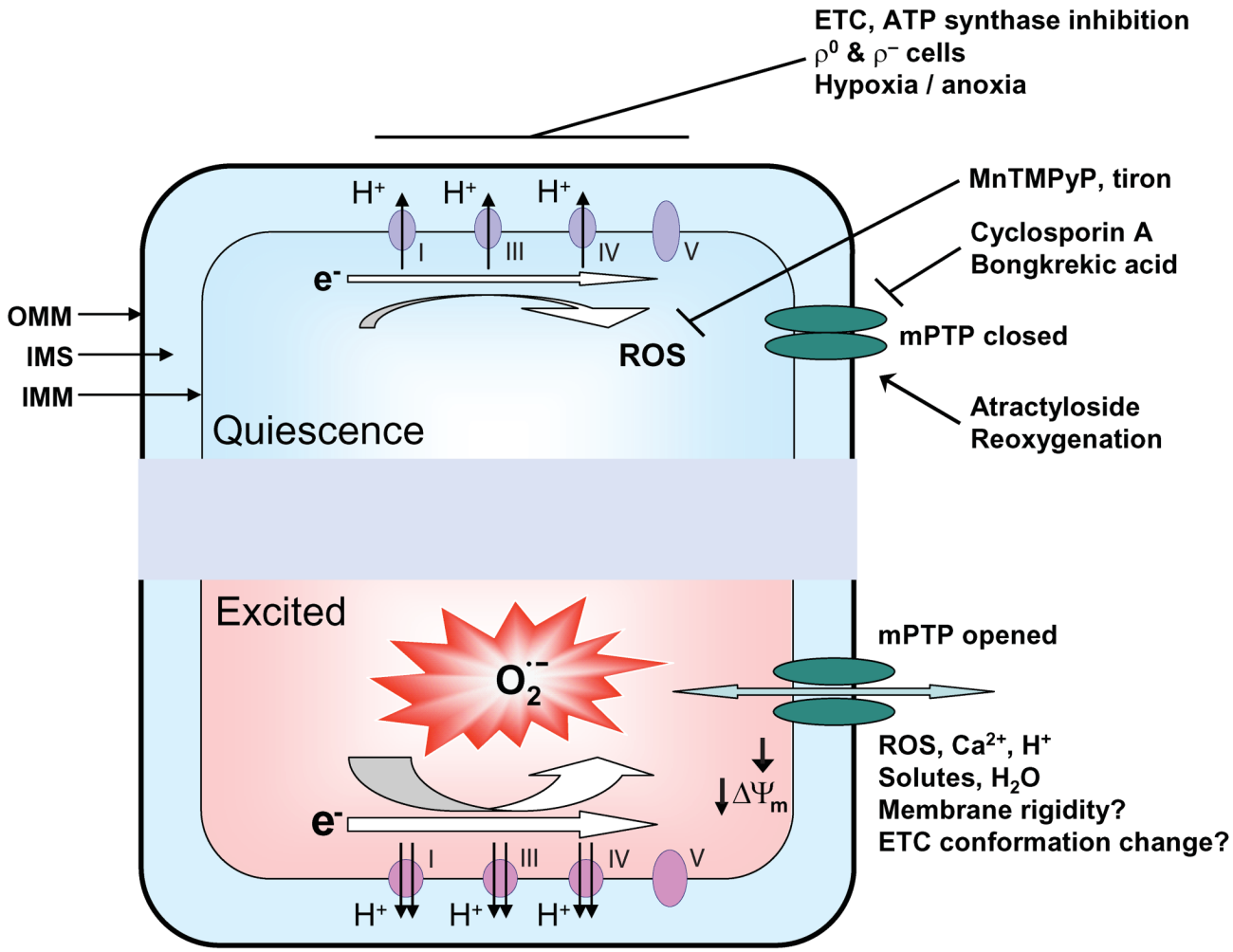

Figure 7. Schematic Model for Superoxide Flash Genesis

In this model, the mPTP opens stochastically in response to physiological ROS levels set by constitutive ROS production by the ETC. Opening of the mPTP causes depolarization of $\Delta\Psi_m$, dissipation of chemical gradients across the inner membrane, and mitochondrial swelling due to water movement as well as changes in inner membrane fluidity and rigidity, which diverts electrons of the ETC to ROS generation. This simple model explains many salient features of superoxide flash activity (e.g., requiring the activities of mPTP, ETC and ATP synthase, all-or-none behavior, sensitive to SOD mimetic and superoxide scavenger) and frequency-dependent modulation by maneuvers that alter mPTP and ETC activities. The model also predicts that superoxide flash incidence is not only an optical readout of physiological mPTP activity in living cells, but also serves as a biomarker of oxidative stress in individual mitochondria. OMM: outer mitochondrial membrane; IMS: intermembrane space; IMM: inner mitochondrial membrane.